



Effect of Surface Active Agents on the Performance of Hydroxiapatite Coating Electrodeposited on Mg-3 Zn-0.8 Ca Alloy

I. M. Ghayad^{1*}, M Shoeib¹, N.N. Girgis¹, H. Soliman¹, S.M. Abd El Hallem²

¹Corrosion Control & Surface Protection Department, Central Metallurgical Research and Development Institute, CMRDI, Cairo, Egypt

²Chemistry Department, Faculty of Science, Zagazig University, Zagazig, Egypt

Received 19 May 2015, Revised 30 July 2015, Accepted 30 July 2015

*Corresponding author. E-mail: ighayad@yahoo.com

Abstract

The effect of different concentrations of both polyethylene glycol (PEG) (0.01-0.2 g/l) and sodium lauryl sulfate (SLS) (0.01-0.1 g/l) on the performance of fluoridated hydroxiapatite (FHA) coating electrodeposited on Mg-0.8 Zn-0.2 Ca alloy was addressed. The FHA coating was evaluated in simulated body fluid (SBF) using open circuit potential, potentiodynamic polarization and electrochemical impedance spectroscopy (EIS) techniques. Surface characterization of the FHA coatings was performed using scanning electron microscopy (SEM) and energy dispersive x-ray spectroscopy (EDS) techniques. Potential measurements during electrodeposition of FHA showed that more stable deposition potential and hence more stable coating growth is exhibited in the presence of PEG. EIS and potentiodynamic measurements revealed that PEG increases the level of passivation of the FHA layer more than SLS. Both additives have resulted in a shift of the E_{corr} to more noble values, more grain refinement of FHA coatings, better compactness and more corrosion resistance. The enhancement mechanism of PEG and SLS was discussed.

Key Words: Mg-Zn-Ca alloys, Hydroxiapatite, electrodeposition, surfactants.

1. Introduction

Studies [1-6] have shown that magnesium alloys possess a promising future as biodegradable implant materials. The biodegradation of magnesium alloys would keep the patient from second surgery. However, the main difficulty to the clinical use of magnesium alloys is their high corrosion rate which induces a mismatch with the bone healing rate and a gap formed between the implant and the surrounding tissue [7]. A controllable corrosion rate combined with biocompatibility plays a key role in the application of magnesium alloys in medical implants. The application of fluoridated hydroxyapatite (FHA) on Mg alloys surfaces renders them bioactive and biocompatible [8,9]. The electrochemical deposition (ED) technique could fabricate a uniform coating on a porous substrate or one with a complex shape and also adjusts the morphology and composition of Ca-P coating easily [10].

The performance of FHA coating on Mg-alloys substrates is improved through the addition of surface active agents to the coating bath. The use of surfactants in coating processes is well known [11-15]. The most popular surfactant sodium dodecyl sulfate (SDS) ($\text{CH}_3(\text{CH}_2)_{11}\text{SO}_4\text{Na}$) was used in the electrodeposition of nano-composite coatings such as Ni-P/SiC, Ni/Al₂O₃, Ni/WC and Ni/CNT. Results have indicated the positive influence of SDS surfactant on uniform distribution of nano-particles [11]. SDS was used to improve the phosphate coating formation on AZ31 magnesium alloy giving more uniform coating with less micro-cracks [11]. The morphology of coating deposited from SDS containing solution showed smooth surface due to columnar growth mode with fine grains [12].

SDS provided a stable condition for one-step electrodeposition of CuInSe₂ thin films. The addition of SDS not only allowed the electrodeposition of more indium in the precursor film but also gave smooth and compact films without pinholes [13].

Polyethylene glycol (PEG) ($\text{HO}-(\text{CH}_2\text{CH}_2\text{O})_n\text{H}$) is a chemical encompassing a polyether backbone that is chemically inert with terminal hydroxyl group. PEG was used as the dispersant during the deposition of HA nanoparticles in isopropanol. It was found that PEG is protonated in isopropanol and then adsorbed on the HA nanoparticles surfaces increasing their stability. PEG in the coatings acted as a binder and prevented their cracking [14].

PEG was also used in targeted drug delivery system because it is non-toxic, non-immunogenic, and non-antigenic. It was coated on the nanoparticle surface to disperse and to reduce the non-specific protein adsorption and clearance by macrophages and to render the nanoparticles capable of crossing the cell membrane [15]. The present paper addresses the effect of additions of sodium lauryl sulfate (SLS) and polyethylene glycol (PEG) surfactants on the performance of FHA coating on Mg-0.8 Zn-0.2 Ca alloy.

2. Materials and methods

2.1. Preparation of Fluoridated Hydroxiapatite coatings

The alloy with a chemical composition of Mg- 3 wt.% Zn- 0.8 wt%. Ca was prepared from pure Mg (99.99%), zinc (99.98%) and Ca (99.98%) using a laboratory resistance furnace under CO₂ and SF₆ protection gases. Zn and Ca were selected as alloying elements because they are essential elements to human body and through optimizing the contents of Zn and Ca, corrosion resistance of the alloy may be improved. The melt was transferred to a semi-continuous casting machine at 650 °C, about 50 °C higher than the liquidus. After casting, power ultrasonic field was applied. The ultrasonic system consists of an ultrasonic generator with a maximum power output of 2 kW and a transducer with a fixed frequency of 20 kHz. Microstructure and grain size of the tested alloy were investigated using optical microscope (Axiovision SE64). Specimens having dimensions of 25×10×4 mm were prepared, polished with SiC papers progressively up to 1000 grits and finally subjected to ultrasonic cleaning in ethanol for 15 min. Prior to FHA coating, samples were anodized in order to improve the coating adherence. During the process of anodizing, the sample was used as the anode. Anodizing was performed in 1N NaOH under voltage of 3V and time 30 min. The electrodeposition of FHA on anodized substrate was carried out in two-electrode cell equipped with graphite plate serving as the counter electrode while the Mg alloy substrate was used as the cathode. The optimum bath composition and operating conditions are given in Table 1. H₂O₂ was introduced to only produce OH⁻ ions on the cathode during the electrodeposition process instead of the usual case which produces H₂ gas. Therefore, H₂O₂ could reduce the effect of H₂ evolution on the nucleation and growth of FHA. After deposition, the specimens were rinsed in distilled water and then dried.

Table 1: Optimum bath composition and operating conditions of the electrodeposition of fluoridated hydroxiapatite coating.

Chemicals	Weight	Role	Operating conditions	
CaNO ₃	0.042 mol/l	Source of Ca ²⁺ ions	Current density	20 mA/cm ²
NH ₄ H ₂ PO ₄	0.025 mol/l	Source of PO ₄ ³⁺ ions	pH	3.8
NaNO ₃	0.15 mol/l	Increase conductivity	Time	30 min
H ₂ O ₂	20 ml/	Erase gas evolution	Agitation	300 rpm
NaF	0.2 g/l	Source of F ⁻ ions	Temperature	Room temperature
Na ₃ PO ₄	2 g/l	Buffer		
PEG	0.01-0.2 g/l	Additive		
SLS	0.01-0.1 g/l	Additive		

2.3. Electrochemical measurements

Electrochemical measurements were performed using a computerized potentiostat (Autolab PG STAT 30) in simulated body fluid (SBF) whose composition was: 8.8 g/l NaCl, 0.4 g/l KCl, 0.14 g/l CaCl₂, 0.35 g/l NaHCO₃, 1.0 g/l C₆H₆O₆ (glucose), 0.2 g/l MgSO₄ 7H₂O, 0.1 g/l KH₂PO₄.H₂O, 0.06 g/l Na₂HPO₄.7H₂O, pH 7.4, at a temperature of 37°C [17]. A conventional three-electrode cell was used in conducting electrochemical tests. Alloy sample, a platinum counter electrode and a saturated calomel electrode were used as the working, counter and reference electrodes; respectively. The area of the working electrode exposed to the solution was 0.196 cm². Potentiodynamic polarization experiments were measured at a scan rate of 0.5 mVs⁻¹ starting from the less to the more noble potentials. The electrodes were preimmersed for 15 min in the testing solution before testing. Electrochemical impedance spectroscopy (EIS) measurements were performed at frequencies ranged from 60 kHz to 10 mHz, and the perturbation amplitude was 5 mV. Surface morphology of tested specimens before and after corrosion tests was carried out using scanning electron microscope (SEM) JEOL, JSM 5410, Japan. Surface analysis was performed using energy dispersive spectroscopy unit attached to the SEM.

3. Results and discussion

3.1. Microstructure investigation

Fig. 1 displays the optical micrographs of the alloy. The microstructure consists of α-Mg matrix and secondary phase of intermetallic compound. The average grain size was about 82 μm.

3.2. Electrochemical measurements

The potential-time variation during FHA deposition process in the presence of PEG or SLS additives is presented in Figures 2,3, respectively. PEG shows initially a rapid decrease in potential followed by an increase till

attaining a steady state value after 600 second. The potential is shifted towards more noble values as the concentration of PEG is increased. The initial decrease in potential is related to FHA coating dissolution in the presence of Mg^{2+} ions which inhibits the coating formation [10]. At the steady state potential coating precipitation is observed which is related to slow nucleation rate resulting in producing smaller number of active sites and gives finer precipitates [14]. On the other hand, SLS surfactant shows unstable potential up to 1200 second. At longer times, the curve shifts fast to more noble potential due to sudden progressive nucleation. The progressive nucleation is related to SLS effect on activating many sites through conductivity enhancement [11-12]. The highest shift in potential is observed at 0.002 g/l SLS.

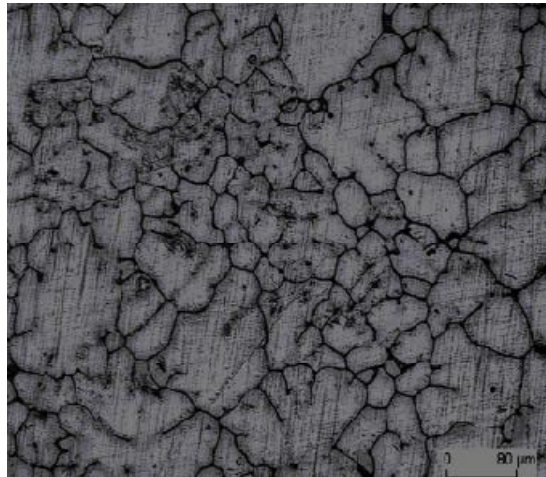


Figure 1. Microstructure of the alloy specimen, X= 100

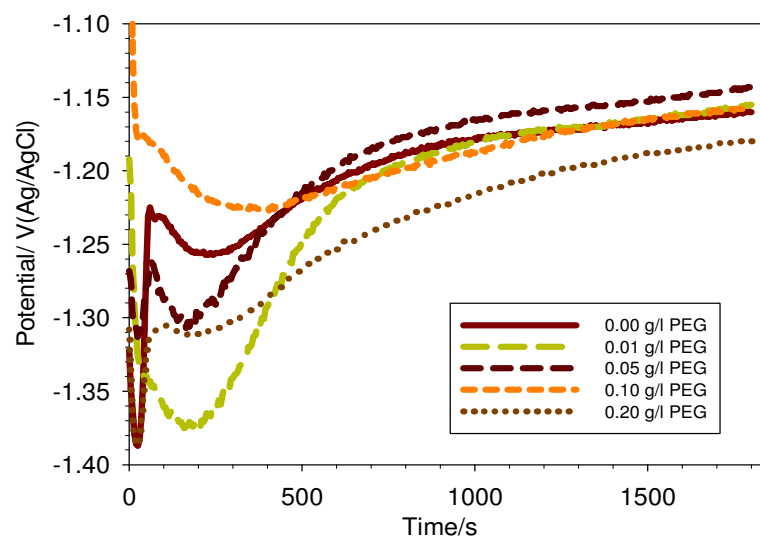


Figure 2: Potential-time curve of FHA coatings in the SBF solution containing different concentrations of PEG compound

The corrosion resistance of the FHA coatings were evaluated in the SBF solution in the absence and presence of different concentrations of PEG and SLS surfactants using electrochemical impedance spectroscopy (EIS) technique. Figure 4 shows the Nyquist plot of the FHA coatings in the presence of different concentrations of PEG. In the Nyquist plot the real part of the impedance is plotted on the X axis and the imaginary part on the Y axis. In this plot the y-axis is negative and that each point on the Nyquist plot is the impedance Z at one frequency [16-18]. Polarization resistances (R_p) of the different FHA coatings were calculated from the Nyquist spectra by subtracting the impedance at the high frequency (left hand side of the Nyquist plot) which represents the solution resistance (R_s) from the impedance at the low frequency (right hand side of the Nyquist plot) which represents the R_p+R_s . This also can be done using the instrument software by fitting the data to an equivalent circuit predetermined in the software.

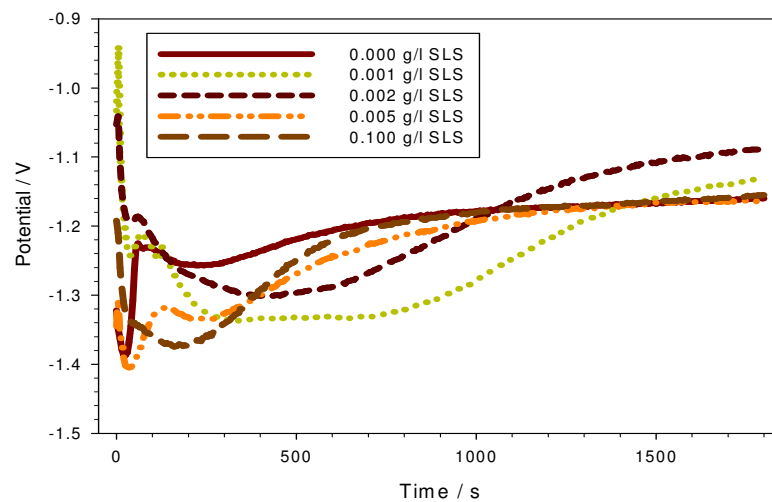


Figure 3: Potential-time curve of FHA coatings in the SBF solution containing different concentrations of SLS compound

The polarization resistance is inversely proportional to the corrosion current (i_{corr}) according to the stern-Geary relationship.

$$R_p = \beta_a \beta_c / 2.3 (\beta_a + \beta_c) i_{corr}$$

where β_a and β_c are the cathodic and anodic Tafel slopes. Equation 4 denotes that there is a direct proportionality between R_p and corrosion resistance.

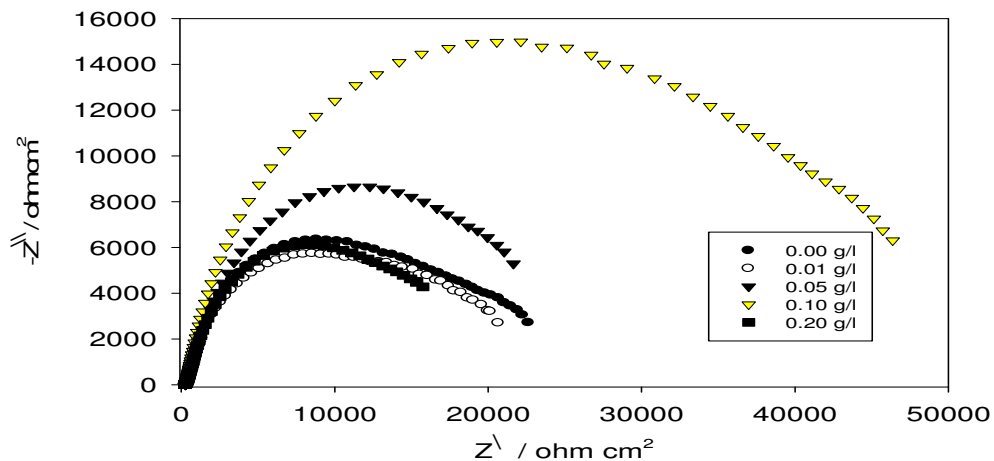


Figure 4: Nyquist plots of FHA coatings in the SBF solution containing different concentrations of PEG compound

Figure 5 shows the R_p values in the absence and in the presence of PEG. The highest R_p (4.6×10^4 ohm) is obtained in the presence of 0.1 g/l PEG which is almost double the R_p obtained in its absence. The Nyquist plot in the presence of SLS is shown in Figure 6. The addition of SLS also enhances the corrosion resistance of the FHA coating. The optimum concentration of SLS, represents the highest increase polarization resistance up to 3.9×10^4 ohm is 0.002 g/l (Figure 7).

Potentiodynamic curves (Figures 8,9) further confirm the previously mentioned results, the PEG additive shifts E_{corr} to more noble values and show rather wide passive region. The highest level of passivation is shown in the presence of 0.1 g/l PEG which shows a passive region of 0.440 V compared to 0.12 V obtained in its absence (Figure 8). On the other hand, potentiodynamic curves in the presence of SLS (Figure 9) show that the additive slightly shifts the corrosion potential (E_{corr}) towards more noble values.

Comparing the corrosion resistance in the presence of either PEG or SLS reveals that PEG is more effective. PEG shows higher R_p , more noble E_{corr} and higher level of passivation which can be related to the stable growth of the insulating FHA layer in the presence of PEG. On the other hand, SLS shows lower enhancement in corrosion resistance due to unstable growth of the FHA layer. In either cases PEG and SLS as anionic surfactants are adsorbed on the micro anodic sites and also prevent magnesium from dissolution. Consequently, the number of microcathodic sites increase leading to more FHA deposition [11-12,14].

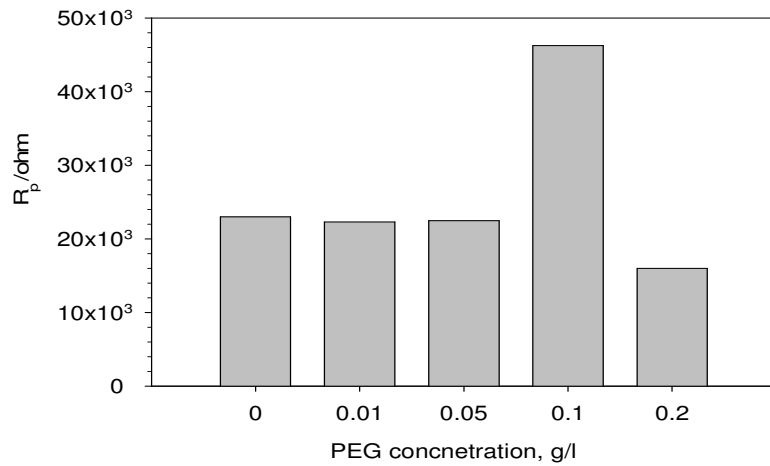


Figure 5: Polarization resistance derived from Nyquist plots of FHA coatings in the SBF solution containing different concentrations of PEG compound

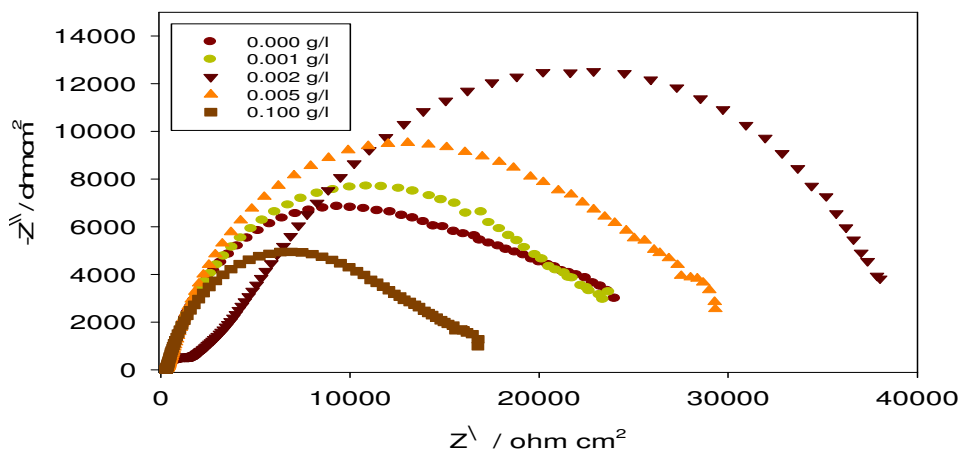


Figure 6: Nyquist plots of FHA coatings in the SBF solution containing different concentrations of SLS compound

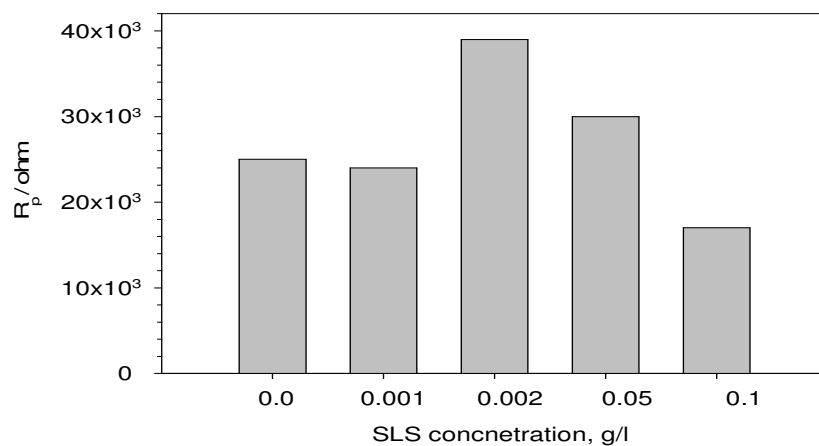


Figure 7: Polarization resistance derived from Nyquist plots of FHA coatings in the SBF solution containing different concentrations of SLS compound

3.3. Coating morphology

The SEM images of FHA coatings deposited in the absence and in the presence of SLS and PEG before and after corrosion are shown in Figures 10,11. The particles of FHA coating deposited from the bath containing PEG are well distributed in the polymer matrix as nano-particles (<50nm). This coating is better than the FHA coating deposited from the bath containing SLS (FHA nano-particles <100 nm). These nano-structure grains of FHA coating indicate that long-chain compound acts as an inhibitor for FHA flakes growth during electrodeposition.

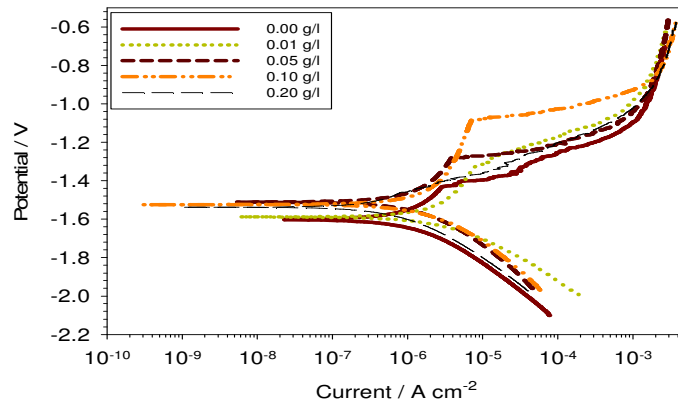


Figure 8: Potentiodynamic curves of FHA coats in the SBF solution containing different concentrations of PEG compound

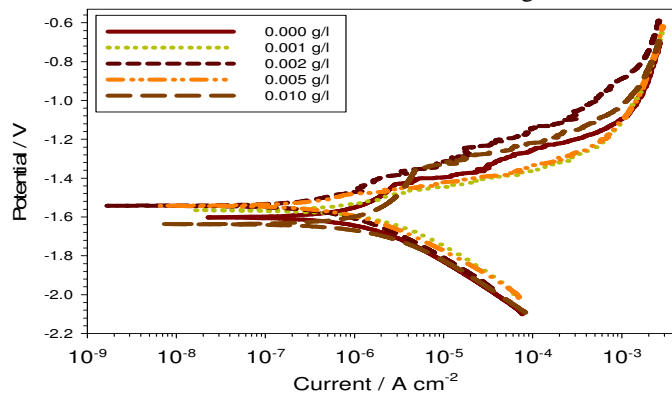


Figure 9: Potentiodynamic curves of FHA coats in the SBF solution containing different concentrations of SLS compound

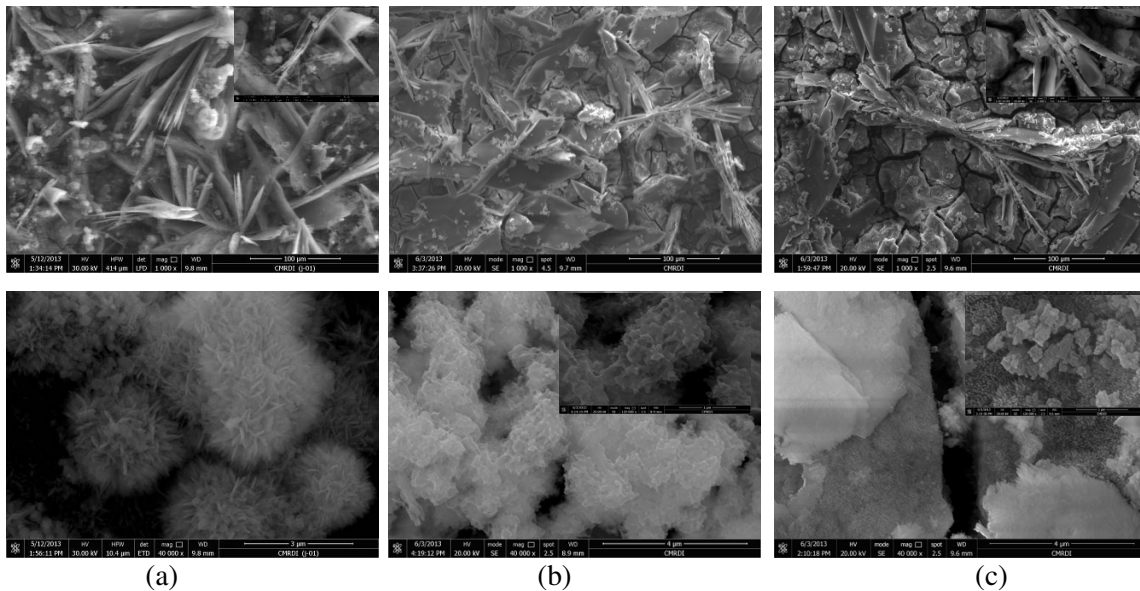


Figure 10: SEM morphology for (a) additive-free (b) PEG-additive (c) SLS-additive coatings before corrosion testing in the SBF solution.

The denser coating with finer particles could be related to stable growth of the deposited coating particles after adsorption on the anionic additives particles. After corrosion testing PEG and SLS give shallow non-deep pits with smaller size (Figure 11). PEG compound with its multi-function groups lead to compact coating formation with nano-particles leading to corrosion resistance enhancement. The presence of both additives results in more grains refinement of coatings, better compactness and higher corrosion resistance till its optimum value. Any more increase in additive concentration hinders ions conductivity and hence coating deposition leading to a drop in coating performance even worse than additive-free FHA coating. These findings demonstrated increased corrosion protection in the presence of both additives compared to additive-free coat.

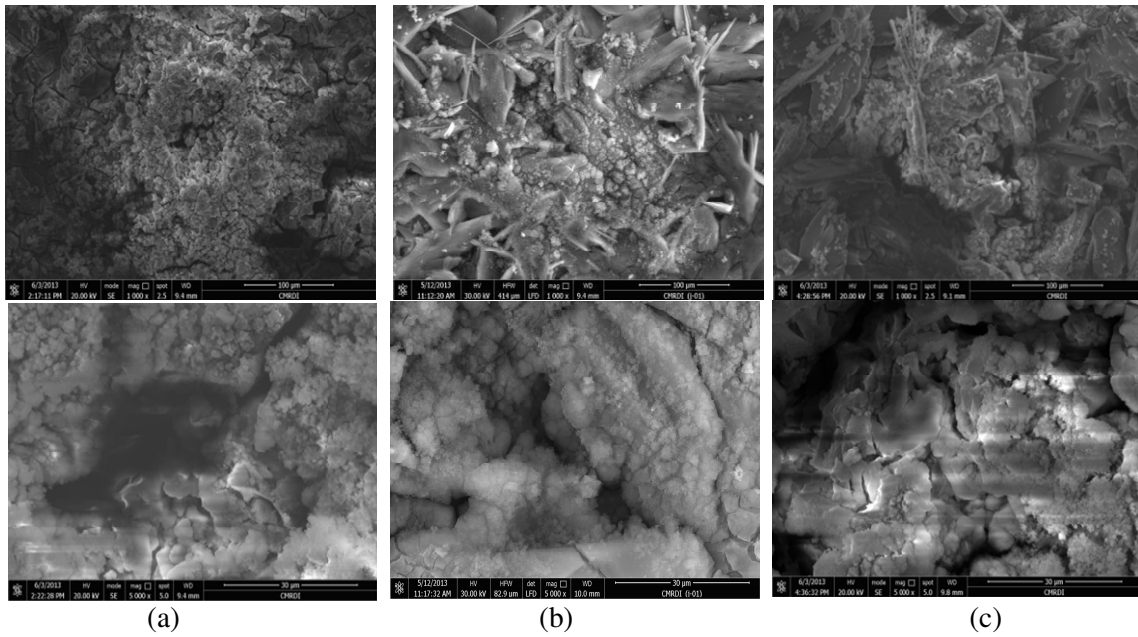


Figure 11: SEM morphology for (a) additive-free (b) PEG-additive (c) SLS-additive coatings after corrosion testing in the SBF solution.

3.4. EDS Results

The EDS spectra of FHA formed in the presence of SLS or PEG additives before and after corrosion test, respectively are presented in Figures 12,13. Before corrosion testing, both additives show better covering for Mg substrate reflected in a reduction of Mg peak. Using PEG produces Ca/P molar ratio of about 1.4 which is closer to the natural bone ratio. On contrast SLS yield Ca-deficient FHA coating with Ca/P molar ratio of 1.1. Therefore, PEG is a beneficial additive for particles refinement and rearrangement keeping the composition of apatite while, SLS leads to fast growth of fine apatite particles but with a lower Ca/P ratio.

After corrosion, both additives give an obvious increase in Mg peak, which is related to coating dissolution, and a reduction in chloride peak indicating better protection of the substrate from aggressive corrosive ions. PEG exhibits no-chloride peak in contrast to SLS that showed chloride peak weaker than that for additive-free FHA coating. Thus, both of the additives enhance coating resistance to corrosive ions.

The present paper denotes the positive impact of surface active agents (PEG and SLS) on the performance of FHA coating electrodeposited on Mg-3 Zn-0.8 Mg substrate. Both materials act as anionic surfactants whose mechanism is illustrated in Fig.14 [11]. The charged molecules are adsorbed on the micro anodic sites (having less electron density). The increase of electron density at the microanodic sites makes them behave as microcathodic sites and thus the rate of coating deposition is increased. On the other hand, the adsorption of charged molecules on the microanodic sites prevents Mg from dissolution.

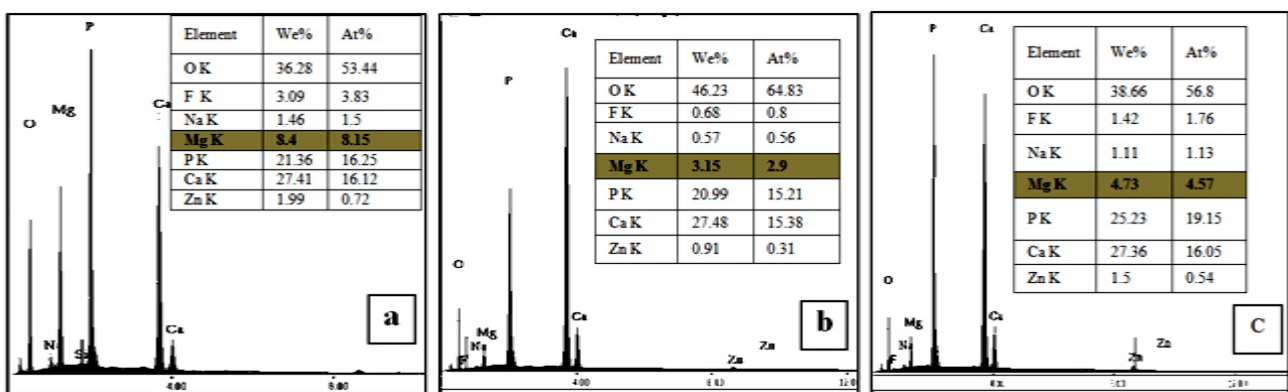


Figure 12: EDS analysis of FAH coating in the absence (a) and in the presence of PEG (b) and SLS (c) before corrosion testing in the SBF solution

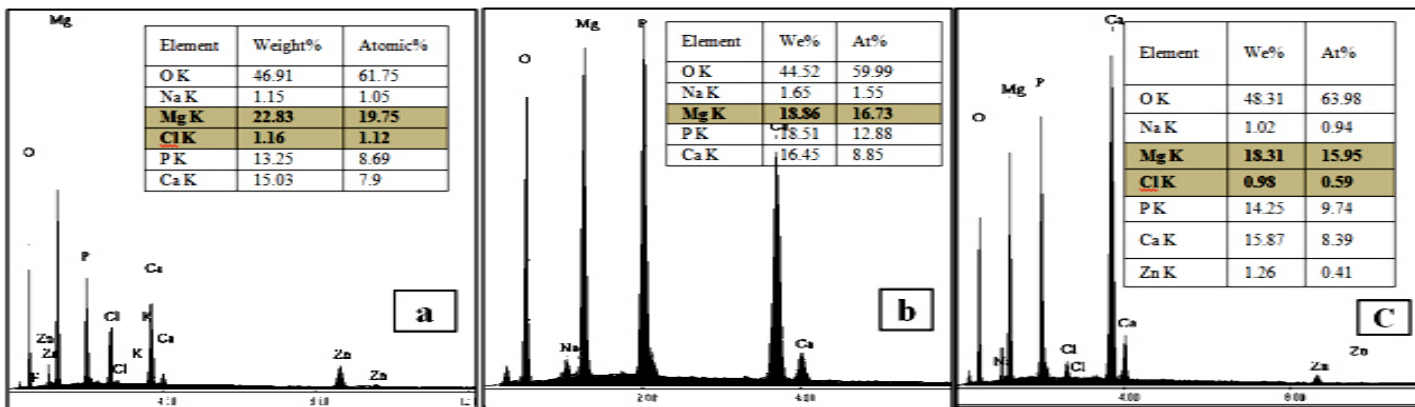


Figure 13: EDS analysis of FHA coating in the absence (a) and in the presence of PEG (b) and SLS (c) after corrosion testing in the SBF solution

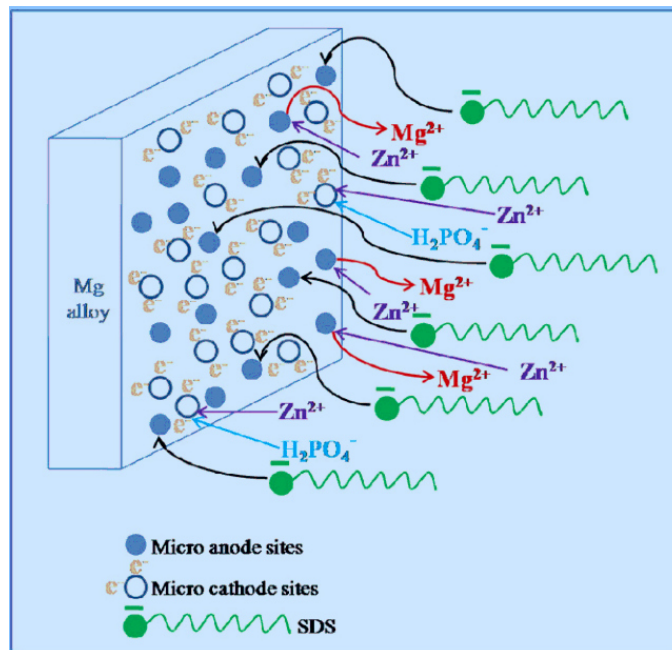


Figure 14: Schematic illustration for charged particles molecules effect on coating deposition on the surface of the Mg alloy. *Amini and Sarabi, Appl. Surf. Sci., 257 (2011) 7134 [11]*

Conclusions

The effect of the addition of long chain surface active agents on the performance of FHA coatings electrodeposited on Mg-3Zn-0.8Ca alloy have been investigated by means of electrochemical measurements, SEM and EDS. The following conclusions can be drawn:

- Impedance and potentiodynamic measurements indicates that both additives increased the corrosion protection of FHA coating. High R_p values were obtained while potentiodynamic curves were shifted to more noble direction. The highest level of passivation was obtained in the presence of 0.1 g/l of PEG and 0.001 g/l SLS, respectively.
- The presence of surfactants results in more grains refinement of coatings, more compactness and more corrosion protection till its optimum value. Any more increase in the additive concentration hinders ions conductivity and hence coating deposition leading to lower resistance even worse than additive-free FHA coating.
- PEG is more effective than SLS which is related to stable growth of the insulating FHA layer. In either cases PEG and SLS as anionic structures are adsorbed on the micro anodic sites preventing Mg from dissolution. Consequently, the number of microcathodic sites increase leading to more FHA deposition.

Acknowledgements - Authors acknowledge the financial support of work by the Egyptian Academy of Scientific Research and Technology.

References

1. Staiger M.P., Pietaka A.M., Huadmaia J., Dias G., *Biomater.* 27 (2006) 1728.
2. Witte F., Kaese V., Switzer H., Meyer-Lindenberg A., Wirth C.J., Windhag, H., *Biomater.* 26 (2005) 3557.
3. Gu X., Zheng Y., Cheng Y., Chong S., Xi, T., *Biomater.* 30 (2009) 484.
4. Hänzi A.C., Gerber, I., Schinhammer, M., Löffler J.F., Uggowitzer, P.J., *Biomater.* 6 (5) (2010) 1824.
5. Zhang S., Zhang, X., Zhao, C., Li, J., Song, Y., Xie, C., Tao, H., Zhang Y., He Y., Jiang, Y., *Acta Biomater.* 6 (2) (2010) 626.
6. Li Z., Gu X., Lou, S., Zheng, Y., *Biomater.* 29 (2008) 1329.
7. Song Y.W., Shan D.Y., Chen, R.S., Zhang F., Han, E.H., *Mater. Sci. Eng. C*, 29 (2009) 1039.
8. Meng E.C., Guan S.K., Wang H.X., Wang L.G., Zhu S.J., Hu J.H., Ren C.X., Gao J.H., Feng Y.S., *App. Surf. Sci.*, 257 (11) (2011) 3811.
9. Wang J., Chao, Y., Wan Q., Zhu, Z., Yu, H., *Acta Biomater.*, 5 (2009) 1798.
10. Liu, G.Y., Hu, J., Ding, Z.K., Wang, C., *Mater. Chem. Phys.*, 130 (2011) 1118.
11. Amini, R., Sarabi, A.A., *Appl. Surf. Sci.*, 257 (2011) 7134.
12. Shirani, A., Momenzadeh M., Sanjabi, S., *Surf. Coat. Tech.*, 206 (2012) 2870.
13. Yu, R., Rem, T., Li, C., *Thin Solid Films*, (518) (2010) 5515.
14. Loghmani, S.K., Farrrokhi-Rad, M., Shahrabi, T., *Cer. Int.* 39 (2013) 7043.
15. Venkatasubbu G.D., Ramasamy S., Avadhani G.S., Ramakrishnan V., Kumar J., *Powder Tech.*, 235 (2013) 437.
16. Bard A.J., Faulkner L.R., *Electrochemical Methods; Fundamentals and Applications*, John Wiley & Sons, New York, 2000, p. 376.
17. Macdonald J.R., *Impedance Spectroscopy: Emphasizing Solid Materials and Systems*, John Wiley & Sons, New York, 1987.
18. Ghayad I.M. and Saad A.Y., *Journal of Metallurgical Engineering (ME)*, 2 (3) (2013) 100.